

Cu gettering in ion implanted and annealed silicon in regions before and beyond the mean projected ion range

R. Kögler, A. Peeva, A. Lebedev, M. Posselt, W. Skorupa, G. Özelt, H. Hutter, and M. Behar

Citation: *Journal of Applied Physics* **94**, 3834 (2003); doi: 10.1063/1.1602951

View online: <http://dx.doi.org/10.1063/1.1602951>

View Table of Contents: <http://scitation.aip.org/content/aip/journal/jap/94/6?ver=pdfcov>

Published by the [AIP Publishing](#)



Re-register for Table of Content Alerts

Create a profile.



Sign up today!



Cu gettering in ion implanted and annealed silicon in regions before and beyond the mean projected ion range

R. Kögler,^{a)} A. Peeva, A. Lebedev, M. Posselt, and W. Skorupa
Forschungszentrum Rossendorf e.V., POB 510119, 01314 Dresden, Germany

G. Özelt and H. Hutter
Technische Universität Wien, Getreidemarkt 9/151, 1060 Wien, Austria

M. Behar
Universidade Federale do Rio Grande do Sul, 91501-970, Porto Alegre, RS, Brazil

(Received 24 February 2003; accepted 26 June 2003)

The strong gettering of Cu atoms in single-crystal Si implanted with 3.5 MeV P⁺ ions is studied after thermal treatment and Cu contamination. Cu decorates the remaining implantation damage. Three separate Cu gettering layers are detected by secondary ion mass spectrometry: at the main projected ion range R_p below R_p ($R_p/2$ effect) and beyond R_p (trans- R_p effect). The defects acting as gettering centers at $R_p/2$ and R_p are implantation induced excess vacancies and excess interstitials, respectively. Cu profiles fit very well with depth distributions of excess vacancies and excess interstitials determined by binary collision simulations for random and channeled ion incidence. The $R_p/2$ effect for P⁺ implantation is found to be significantly reduced in comparison with Si⁺ implantation. It disappears completely for higher P⁺ ion fluences. The trans- R_p gettering layer is formed by thermal treatment. The Cu accumulation in the trans- R_p region increases with increasing temperature and/or with increasing annealing time. These results are in qualitative agreement with the assumption that interstitials carried by P diffusion are the origin of Cu gettering in the trans- R_p region. The P diffusion may inject interstitials into the bulk and also into the $R_p/2$ region thus decreasing the $R_p/2$ effect. © 2003 American Institute of Physics.
[DOI: 10.1063/1.1602951]

I. INTRODUCTION

A few years ago, the Cu metallization technology was introduced in advanced microelectronics device structures. However, Cu and other transition metals are known to deteriorate the device characteristics if they are present in active device areas.¹ Therefore, special interest has arisen regarding the Cu redistribution during thermal processes and the Cu trapping by device structures and crystal damage. Implantation-induced damage very effectively traps impurities in Si also after annealing at relatively high temperatures.² Defects in Si can be detected by taking the accumulation of an impurity like Cu in a certain region as a tracer for defects in this region. In this way a new defective layer in ion implanted and annealed Si was discovered almost at about half of the mean projected ion range, R_p .³⁻⁵ The corresponding gettering effect was termed “ $R_p/2$ ” effect.⁶ The origin of the defects at $R_p/2$ has been a subject of discussion as there was no undoubted evidence for the defects by any other analysis method.⁷⁻⁹ Meanwhile implantation induced excess vacancies at $R_p/2$ were proven to be the dominating gettering centers for Cu atoms. Excess vacancies before R_p and excess interstitials at R_p are generated during the process of ion implantation by the spatial separation of vacancies (V) and interstitials (I).⁷ It was demonstrated that the $R_p/2$ gettering effect can be suppressed either

by ion implantation under an inclined incidence angle or by an additional implant of Si⁺ ions into the excess vacancy containing region.^{10,11} Both the incidence angle and the fluence of the additional implant just necessary to avoid the $R_p/2$ effect were found to be in agreement with the excess vacancy model. Moreover, an enhanced depth resolution of positron annihilation spectroscopy and an improved specimen preparation for transmission electron microscopy (TEM) made it possible to detect very small cavities, the agglomerates of excess vacancies in ion implanted and annealed Si.¹²⁻¹⁵ More recently, the separation of depth profiles of vacancy-related and interstitial-related defects in the as-implanted state was observed by the deep level transient spectroscopy utilizing the filling pulse technique.¹⁶ The excess vacancy generation at $R_p/2$ during ion implantation is assumed to be a general phenomenon of ion implantation. However, we are far away from a real understanding of all processes of damage production during ion implantation and of damage annealing during thermal treatment. Replacing the implanted Si⁺ ion by a P⁺ ion, a common dopant in Si with similar ion mass, leads to different gettering effects. For P⁺ and As⁺ ion implantation Gueorguiev *et al.*^{17,18} reported the formation of another gettering layer beyond R_p . This gettering effect called “trans- R_p ” gettering cannot be explained in terms of the excess vacancy model. Interstitial clusters were suggested to be the origin of these gettering centers and Cu gettering in the region beyond R_p was correlated to the diffusion mechanism of the dopants P and As in Si.^{17,18} How-

^{a)}Electronic mail: Koegler@FZ-Rossendorf.de

ever, there is no proof up to now that interstitial clusters are present at the depth beyond R_p acting as gettering centers for an impurity like Cu.

The aim of the present article is to investigate in more detail Cu gettering after P^+ ion implantation and subsequent annealing. Special emphasis is given to a comparison of the formation conditions of the $R_p/2$ gettering (before R_p) and the trans- R_p gettering (beyond R_p). All implantation and annealing conditions are varied which are known to have an effect on the Cu gettering at $R_p/2$. Such parameters are ion fluence, ion incidence angle, annealing temperature, annealing time, and the cooling rate of the last thermal process step. Ion channelling is especially investigated, it is a process which potentially may effect the defect structure at the depth beyond R_p .

II. EXPERIMENT

3.5 MeV P^+ ions were implanted into (100)-oriented, n -type CZ-Si for ion fluences, Φ , between 5×10^{14} and $5 \times 10^{15} \text{ cm}^{-2}$. Ion incidence angles of 7° and 55° were chosen in order to compare different formation conditions of the $R_p/2$ and the trans- R_p gettering layer. Moreover, the formation of the $R_p/2$ gettering layer was studied under the conditions of ion channeling. For ion channeling the equipment of the Federal University of Rio Grande do Sul, Porto Alegre, Brazil was used. In this case ion implantation was performed in the unscanned mode. After implantation the wafers were cut into small samples and subjected to annealing at temperatures between 900 and 1100 °C in an Ar ambient by either rapid thermal annealing (RTA) for 5 or 30 s or by furnace annealing for 30, 60, or 180 min. Subsequently, the samples were contaminated with a low amount of Cu by implanting the impurity atoms at 20 keV to a fluence of $3 \times 10^{13} \text{ cm}^{-2}$ on the backside and processed by a thermal treatment (RTA) at 700 °C for 180 s to redistribute the Cu atoms throughout the wafer bulk toward the gettering layers. The controlled cooling rate of this annealing was held constant at 5 K/s. For one sample an additional post-annealing at 880 °C for 10 min and a final quenching (cooling rate ≥ 100 K/s) was performed using a special home-made furnace at the University of Halle, Germany.

The depth profiles of P, Cu, and other impurities (C,O) in Si were measured by secondary ion mass spectrometry (SIMS). The defect structure formed after implantation and annealing was studied by cross section transmission electron microscopy (XTEM) with improved resolution. XTEM specimens were prepared by conventional ion milling as well as by cleaving. The cleaving technique, a special method for TEM specimen preparation, avoids the damage generation as introduced by conventional specimen thinning. For Si^+ implantation the cleaving technique has been successfully applied to visualize very small cavities at $R_p/2$ with diameters of about 2 nm.^{14,15} Carrier concentration depth profiles in the samples were determined by the spreading resistance profiling (SRP) technique.

III. SIMULATION

Excess vacancies and excess interstitials are defects which remain after complete local recombination of implantation-induced Frenkel pairs ($I+V$).¹⁹ Their generation during the process of implantation was simulated by the binary collision code TRIM (transport of ions in matter).^{7,11} However, TRIM considers only amorphous target structures. It cannot treat channeling effects occurring in ion implantation into single-crystalline Si (c -Si). Therefore, in the present article the Monte Carlo engine of the process simulator of Integrated Software Engineering, Inc., is employed.²⁰ This computer code originates basically from the Crystal-TRIM program calculating the ion implantation into c -Si.^{21,22} Crystal-TRIM allows the treatment of channeling phenomena. Using the full-cascade feature of Crystal-TRIM accurate ballistic point defect (I,V) profiles can be obtained by the calculation of the trajectories of recoil particles. The dechanneling of ions and recoils due to the damage buildup during irradiation is described by a phenomenological model which is elucidated in detail elsewhere.^{21,22} Below a threshold (C_{crit}) the probability (P_d) that an ion or recoil collides with a target atom of a damaged region depends linearly on the nuclear energy deposition per atom (E_n) in that region. Above the threshold, P_d is set to one, i.e., the target region considered is fully amorphized.

$$P_d = \begin{cases} C_{acc} E_n & C_{acc} E_n \leq C_{crit} \\ 1 & C_{acc} E_n > C_{crit} \end{cases} \quad (1)$$

The 3.5 MeV P^+ implantation was simulated for two conditions: (i) 0° tilt (channeling incidence) and (ii) 7° tilt, 23° rotation (random incidence). In the first and second case the P^+ ion fluence was 2.42×10^{15} and $1.13 \times 10^{15} \text{ cm}^{-2}$, respectively. These data correspond to the values measured by SIMS. In order to obtain a good agreement between measured and calculated P profiles, only one simulation parameter C_{acc} had to be changed from 0.2 (standard value) to 0.05. The reason for this modification is not completely clear. It might be due to the heating of the target during the MeV implantation which may lead to a reduction of implantation damage, and, therefore to a decrease of the value of C_{acc} .

IV. RESULTS

Figure 1 shows Cu profiles for 1×10^{15} and $2 \times 10^{15} \text{ P}^+ \text{ cm}^{-2}$ after annealing at temperatures of 900 and 1000 °C. The three gettering layers at $R_p/2$, R_p , and trans- R_p are clearly visible after thermal treatment at 900 °C for 30 s. At higher temperatures [Fig. 1(a)] or for longer annealing times [Figs. 1(a) and 1(b)] the $R_p/2$ effect disappears. Instead, Cu gettering in the trans- R_p is observed. The trans- R_p effect dramatically increases for the longer annealing time of 30 min and is in general more pronounced for lower P^+ fluences. The measured P profiles displayed in Fig. 1(a) demonstrate how annealing corresponds to P profile broadening. For the lower fluence of $5 \times 10^{14} \text{ P}^+ \text{ cm}^{-2}$ the fraction of Cu trapped at the different gettering layers after annealing at $T=900$ °C is presented in Table I. The amount of Cu in the $R_p/2$ gettering layer is found to be rather small (except the value for 5 s), whereas the main fraction of Cu is distrib-

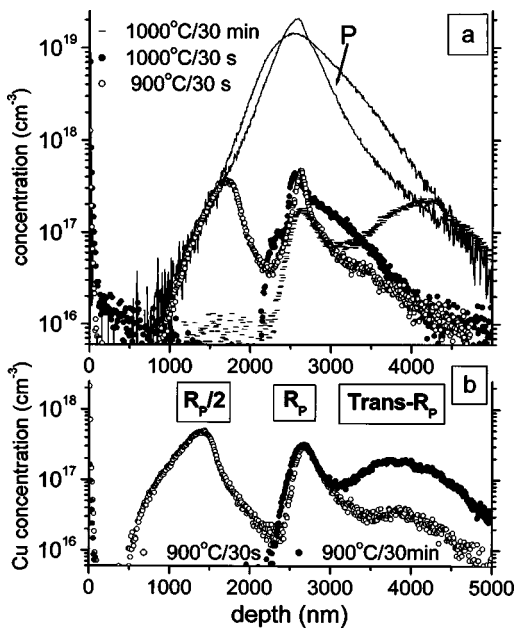


FIG. 1. Cu depth distributions measured by SIMS for 3.5 MeV implants of $1 \times 10^{15} \text{ P}^+ \text{ cm}^{-2}$ (a) and $2 \times 10^{15} \text{ P}^+ \text{ cm}^{-2}$ (b) after annealing and Cu contamination. Three separate gettering layers at $R_p/2$, R_p , and $\text{trans-}R_p$ are formed. To demonstrate the P diffusion, two P profiles are included in Fig. 1(a) corresponding to annealing for 30 s at temperatures of 900 and 1000 °C.

uted in the R_p and $\text{trans-}R_p$ gettering layer. The Cu fraction in the R_p layer decreases and the Cu fraction in the $\text{trans-}R_p$ layer increases with longer annealing times. Quenching of the sample leads to another distribution of Cu with an increased Cu fraction in the R_p layer. For long annealing times the low amount of Cu at $R_p/2$ and R_p may be partly related to gettering of O, knocking Cu atoms out of the gettering site. Such an effect was revealed for Cu atoms gettered at $R_p/2$.^{23,24} Gettering of O in the $\text{trans-}R_p$ region was not observed in our study. The defect structure and the corresponding Cu profile for the implant of $1 \times 10^{15} \text{ P}^+ \text{ cm}^{-2}$ after annealing at 900 °C for 30 min is demonstrated in Fig. 2. For all investigated samples the XTEM images show only dislocation loops at R_p and few elongated dislocations on (111) planes extended from the R_p region into the $\text{trans-}R_p$ region as displayed in Fig. 2(b). The dislocations cannot be the gettering centers at $\text{trans-}R_p$, as such defects were observed also for Si^+ implantation where no $\text{trans-}R_p$ effect occurs.^{17,18} Cavities could be resolved only in the single case

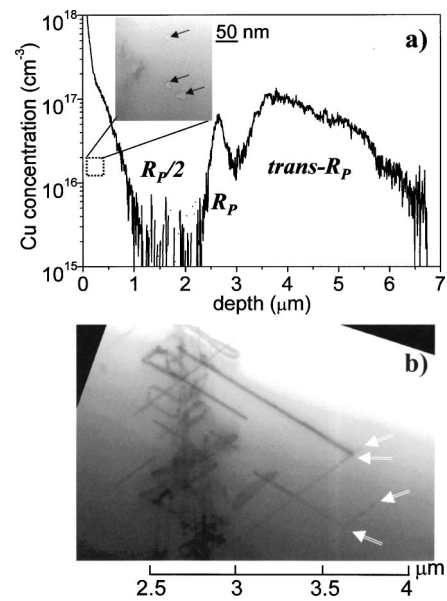


FIG. 2. Cu depth distribution (a) and corresponding bright field XTEM image (b) showing dislocation loops in the region around R_p and some extended dislocations ending in the $\text{trans-}R_p$ region (arrows) as determined for the 3.5 MeV implant of $1 \times 10^{15} \text{ P}^+ \text{ cm}^{-2}$ after annealing at 900 °C for 30 min and subsequent Cu contamination. The inset in Fig. 5(a) shows cavities (marked by arrows) in an underfocus bright field XTEM image taken under kinematical conditions. They were found only in the indicated region close to the surface.

shown in the insert in Fig. 2(a). Very rare cavities were found in the indicated surface-near region. However, no cavities were observed in the region around $R_p/2$. This result is commensurate with the Cu profile of Fig. 2(a) which does not show the typical $R_p/2$ effect visible in Fig. 1. Cavities were not seen in the P^+ implanted samples despite, the observation of the $R_p/2$ effect (Fig. 1). Probably the cavities were too small (diameter ≤ 2 nm) to be detected. Figure 3 shows Cu and P profiles for the higher fluence of $5 \times 10^{15} \text{ P}^+ \text{ cm}^{-2}$. The target was not amorphized during ion implantation. No $R_p/2$ effect and only very small Cu gettering in the $\text{trans-}R_p$ region was observed. The missing $R_p/2$ effect is in contrast to the results of Si^+ implantation. The samples implanted with 3.5 MeV Si^+ ions to a fluence of $5 \times 10^{15} \text{ cm}^{-2}$ clearly demonstrate the $R_p/2$ effect after annealing at 900 °C.^{5,10,11} Figure 4 shows the calculated excess defect profiles ($I-V$) compared with Cu profiles measured for P^+ ions implanted in random and channeled direction

TABLE I. Fraction of Cu found at three gettering layers for 3.5 MeV P^+ implant of $5 \times 10^{14} \text{ cm}^{-2}$ after annealing at 900 °C for different times. The sample annealed for 30 min was post-annealed for 10 min and quenched. Data of the corresponding Si^+ implant are given for comparison.^{a)}

Annealing time at 900 °C	Cu at $R_p/2$	Cu at R_p	Cu at $\text{trans-}R_p$	O gettering	Cu gettering for Si^+ implant
5 s	$\geq 75\%$	$\leq 12\%$	$\leq 12\%$	no	—
30 s	$\leq 2\%$	56%	42%	no	99% at R_p
30 min	$\leq 1\%$	13%	86%	no	97% at R_p
40 min + quenching	$\leq 1\%$	44%	43%	at R_p	—
60 min	—	3%	97%	at R_p	—
180 min	—	$\leq 1\%$	99%	at $R_p/2$ and R_p	—

^{a)}See Ref. 18.

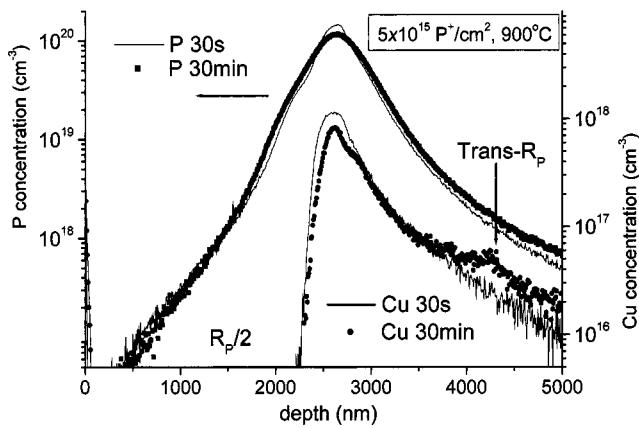


FIG. 3. P depth distributions (left scale) and Cu profiles (right scale) measured by SIMS for 3.5 MeV ions implanted with a fluence of $5 \times 10^{15} \text{ P}^+ \text{ cm}^{-2}$ after annealing at 900°C and Cu contamination. No $R_p/2$ effect is observed.

after annealing at 900°C for 30 s. The calculated data points in the upper part of Fig. 4 with $(I-V) \leq 0$ indicate a vacancy excess whereas the data points with $(I-V) \geq 0$ indicate an excess of interstitials. For both random and channeling implantation, the calculated $(I-V)$ profile as well as the Cu profile results in only two damaged regions, the $R_p/2$ and the R_p layer. The damage created by ion channeling is restricted to the depth range $x \leq 4 \mu\text{m}$. It does not explain the defects indicated by the deeper trans- R_p gettering layer at $x \geq 4 \mu\text{m}$ observed after annealing (Figs. 1 and 2). The number of excess interstitials generated by P^+ implantation depends on whether or not the implanted P atoms finally occupy a lattice site and generate an interstitial (+1). The excess defect distributions $(I-V)$ for the case that all P atoms are on lattice sites (labeled “+1”) were calculated by adding the simulated P profiles. The $(I-V)$ curves displayed in Fig. 4 correspond to the extreme cases that all P atoms are either on interstitial or on substitutional site. P located on a lattice site is electrically active and contributes to the elec-

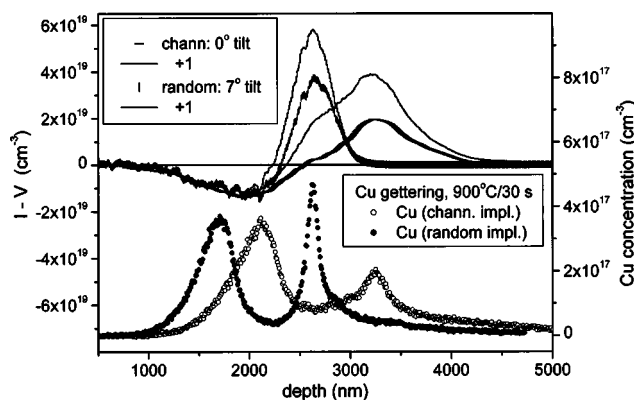


FIG. 4. Comparison of calculated excess defect profiles $(I-V)$ generated by 3.5 MeV, P^+ ion implantation into Si (left scale), and corresponding Cu profiles (right scale). The excess defect profiles (upper part) are shown for random and channeling implantation and for the case that the implanted P^+ ion finally occupies a lattice site (labeled “+1”). The Cu profiles were measured by SIMS after P^+ ion implantation in channeling direction and with random ion incidence subsequent to annealing at 900°C for 30 s and Cu contamination.

tron concentration in n -Si as measured by SRP. The measurement shows that for the implant of $1 \times 10^{15} \text{ P}^+ \text{ cm}^{-2}$ after annealing at $T = 900^\circ\text{C}$ for 30 s a fraction of about 25% of P is not located on lattice sites. Full activation of P was achieved for annealing times $t \geq 100$ s.

V. DISCUSSION

It has to be considered that excess vacancies and excess interstitials are mobile and may recombine during annealing, especially in the region around x_J , the depth where the vacancy excess changes to the excess of interstitials. Diffusion is not taken into account by the simulation. The total amount of excess vacancies (V_E) generated by one P^+ ion can be calculated by the integration of the $(I-V)$ profile in the limits between 0 and x_J . The values V_E and x_J decrease as P occupies lattice sites (“+1” curves in Fig. 4). For both implants, channeled and random ion incidence, the position of the maximum of the calculated excess interstitial profile accurately agrees with the gettering layer of Cu at R_p . However, the Cu profile maximum at $R_p/2$, for random ion incidence in Fig. 4 deviates from profile maximum of the excess vacancies at $x = 2 \mu\text{m}$. The deviation can be explained by the diffusion-assisted I/V recombination which effects more the excess vacancy distribution than the excess interstitial distribution. The very steep $(I-V)$ profile of the random implant in the transition region around x_J results in a stronger diffusive broadening as compared with the case of the channeled implant. This leads to a narrower excess vacancy profile at smaller depth. In summary, there is no evidence that ion channeling is the origin of the additional damage layer beyond R_p which is indicated by the trans- R_p effect.

Gueorguiev et al.^{17,18} suggested that the interstitialcy mechanism of P diffusion, leading to injection and supersaturation of interstitials in the wafer bulk, and their clustering, is responsible for the formation of the separate damage layer beyond R_p , and hence for the trans- R_p effect. The process might be closely related to the so called “emitter-push” effect observed for high concentration P diffusion.²⁵ The P diffusion process was found to getter Au without the formation of dislocations.²⁶ The Cu gettering in the trans- R_p region of a P implant was related to P diffusion derived of SRP measurements.^{17,18} A ratio of $\text{P}/\text{Cu} = 25$ was determined which means that 25 diffusing P atoms are necessary for gettering of one Cu atom in the trans- R_p region.¹⁷ The P/Cu ratios determined from our SIMS data analysis deviate significantly from this value. The P profiles in Fig. 1(a) show an amount of about $3.4 \times 10^{14} \text{ P cm}^{-2}$ diffused into the bulk toward the trans- R_p region. For annealing at 1000°C , 30 s it results in a ratio of $\text{P}/\text{Cu} = 55$, whereas the ratio is $\text{P}/\text{Cu} = 15$ for annealing at 1000°C , 30 min. The variation of the P/Cu ratio is no surprise in view of the rather complex processes leading to Cu gettering in the trans- R_p region. The diffusion of interstitials, their agglomeration, and the defect formation in the R_p region play an essential role. The P-diffusion induced carrying of interstitials and their supersaturation and agglomeration was studied by Uematsu.²⁷ He reported the reduction of the interstitial concentration at the maximum of P concentration (R_p) and the corresponding

TABLE II. Summary of the trends of Cu gettering for two different processes: Cu gettering at the $R_p/2$ layer after Si^+ implantation and Cu gettering at the trans- R_p layer after P^+ implantation. Meaning of the symbols: \uparrow enhanced, \downarrow decreased, \Rightarrow no effect.

Process/dependency		Cu gettering at $R_p/2$ for Si^+ implants	Cu gettering at trans- R_p for P^+ implants
Ion fluence	\uparrow	\uparrow	\downarrow
Ion incidence angle	\uparrow	\downarrow	\Rightarrow
Annealing (temperature, time)	\uparrow	\downarrow	\uparrow
Annealing at $T=1100^\circ\text{C}$		\downarrow	\Rightarrow
Cooling rate	\uparrow	\downarrow	\downarrow

enhancement of the interstitial concentration in the bulk ($2R_p$).

A very important feature of our results is the lack of the $R_p/2$ effect in Fig. 3. The gettering behavior of P^+ and Si^+ implants was found to be different despite the damage induced by Si^+ and P^+ ions is very similar. There should be another process decreasing the number of excess vacancies and the size of their agglomerates which operates in the case of P^+ implantation. This process could be the P diffusion. P diffusing in Si is a carrier of additional interstitials.^{17,18,27} The implanted P profile is broadened by diffusion toward both sides, into the Si bulk and toward the surface. For instance, the P profiles in Fig. 1(a) show an amount of $1.1 \times 10^{14} \text{ P cm}^{-2}$ diffused toward the $R_p/2$ region. A significant fraction of the total amount of excess vacancies (about $2.5 \times 10^{14} \text{ cm}^{-2}$) can recombine in this manner. For higher P^+ fluences the recombination of excess vacancies may be more effective as the P concentration in the whole $R_p/2$ region increases. This is in agreement with the XTEM results (Fig. 2). Cavities were observed only for the implant of $1 \times 10^{15} \text{ P}^+ \text{ cm}^{-2}$ in the region close to the surface ($x \leq 0.5 \mu\text{m}$) where the P concentration is very low [see Fig. 1(a)]. The missing $R_p/2$ effect for increased temperature [Fig. 1(a)] or longer annealing times [Fig. 1(b)] proves that the vacancy defects were annealed out. If they were present, Cu would be trapped there due to the higher binding energy with Cu in comparison to binding with gettering centers at R_p .²⁸ The weak Cu gettering at $R_p/2$ for the P^+ implant of $5 \times 10^{14} \text{ cm}^{-2}$ (Table I) is in agreement with our results for Si^+ implantation showing no $R_p/2$ effect if the calculated average of excess vacancy concentration ($V_E \Phi / x_f$) is below a threshold value of $2 \times 10^{18} \text{ cm}^{-3}$.^{10,11,23} As this threshold value is exceeded, the $R_p/2$ effect appears, for instance, for the implant of $1 \times 10^{15} \text{ P}^+ \text{ cm}^{-2}$ (Fig. 1). The $R_p/2$ effect of O contained in CZ-Si was reported for P^+ implantation and annealing at 1000°C for 1 h.³ O precipitation is another competitive process consuming excess vacancies. For Si^+ implantation the Cu gettering at R_p and $R_p/2$ was found to be completely reversible by applying repetitive thermal treatments and the gettering centers were stable during annealing at $T=900^\circ\text{C}$.²⁸ This condition does not seem to hold in general for P^+ implantation [Fig. 1(b)], but it is approximately correct for Cu trapping in the R_p and trans- R_p region. Table I shows the increase of the trans- R_p effect during annealing and a corresponding decrease of the Cu gettering at R_p . The opposite behavior of Cu gettering at the R_p and trans- R_p layer after a low and high cooling rate demonstrated

in Table I is similar to the gettering behavior of Cu at the R_p and $R_p/2$ layer as observed for Si^+ implantation. Koveshnikov and Kononchuk²⁸ explained the redistribution of Cu from $R_p/2$ to R_p after quenching by the higher trapping probability of Cu at R_p and, on the other hand, by the higher binding energy of Cu at gettering sites in the $R_p/2$ region. A higher trapping probability results from the higher concentration of gettering sites and/or their larger capture cross section. The same arguments may be accepted for Cu gettering at R_p and in the trans- R_p region.

Cu gettering at one gettering layer in accordance with gettering at another one cannot be a predetermination of the same character of gettering centers in both layers and vice versa. However, Table II summarizes that Cu gettering at $R_p/2$ and in the trans- R_p region have different trends with regard to all cases of parameter variation, except the cooling rate. Therefore, it may be assumed that the character of the gettering centers is different in both layers. Vacancy-type defects are known to be gettering centers of the $R_p/2$ layer. The gettering centers in the trans- R_p region may be interstitial-type defects.

IV. CONCLUSIONS

Cu atoms intentionally introduced in ion-implanted Si decorate the remaining implantation damage after annealing. Three different gettering layers are formed. The Cu gettering at $R_p/2$ and R_p was shown to be implantation induced and corresponds to excess vacancies and excess interstitials, respectively. Cu profiles measured after annealing at 900°C for 30 s fit very well the calculated depth distributions of excess vacancies and excess interstitials. The $R_p/2$ effect for P^+ implantation is significantly reduced in comparison with Si^+ implantation. For higher fluences ($5 \times 10^{15} \text{ P}^+ \text{ cm}^{-2}$) the $R_p/2$ effect disappears completely. On the other hand, the trans- R_p gettering layer is formed by thermal treatment. The amount of Cu accumulated in the trans- R_p region increases with increasing temperature and/or with increasing annealing time. The redistribution of Cu toward the R_p gettering layer for high cooling rates can be interpreted in the way that the density of gettering centers in the trans- R_p region is significantly lower than at R_p . TEM revealed no defects beyond R_p except few dislocations extending from R_p into the trans- R_p region. Cu gettering in the trans- R_p region proceeds in a different way compared to Cu gettering by implantation induced excess vacancies at $R_p/2$. These results are in qualitative agreement with the assumption that the gettering centers

for Cu in the trans- R_p region are interstitial clusters formed by P-diffusion induced supersaturation and agglomeration of interstitials. The P diffusion may inject interstitials into the bulk and also into the $R_p/2$ region thus decreasing the $R_p/2$ effect.

ACKNOWLEDGMENTS

The authors gratefully acknowledge R. Krause-Rehberg for quenching of samples after thermal treatment and D. Panknin for performing of SRP measurements. This study was supported by Deutsche Forschungsgemeinschaft (DFG) under Project No. Ko 1287/3-1.

- ¹A. A. Istratov and E. R. Weber, *Appl. Phys. A: Mater. Sci. Process.* **66**, 123 (1998).
- ²H. Wong, N. W. Cheung, P. K. Chu, J. Liu, and J. W. Mayer, *Appl. Phys. Lett.* **52**, 1023 (1988).
- ³M. Tamura, T. Ando, and K. Ohya, *Nucl. Instrum. Methods Phys. Res. B* **59**, 572 (1991).
- ⁴A. Agarwal, K. Christensen, D. Venables, D. M. Maher, and G. A. Rozgonyi, *Appl. Phys. Lett.* **69**, 3899 (1996).
- ⁵R. Kögler, M. Posselt, R. A. Yankov, J. R. Kaschny, W. Skorupa, and A. B. Danilin, *Mater. Res. Soc. Symp. Proc.* **469**, 463 (1997).
- ⁶R. Kögler, R. A. Yankov, J. R. Kaschny, M. Posselt, A. B. Danilin, and W. Skorupa, *Nucl. Instrum. Methods Phys. Res. B* **147**, 96 (1999).
- ⁷R. A. Brown, O. Kononchuk, G. A. Rozgonyi, S. Koveshnikov, A. P. Knights, P. J. Simpson, and F. Gonzalez, *J. Appl. Phys.* **84**, 2459 (1998).
- ⁸A. Peeva, R. Kögler, P. Werner, A. A. D. de Mattos, P. F. P. Fichtner, M. Behar, and W. Skorupa, *Nucl. Instrum. Methods Phys. Res. B* **161–163**, 1090 (2000).
- ⁹R. Kögler, A. Peeva, W. Anwand, G. Brauer, W. Skorupa, P. Werner, and U. Gösele, *Appl. Phys. Lett.* **75**, 1279 (1999).

- ¹⁰R. Kögler, A. Peeva, P. Werner, W. Skorupa, and U. Gösele, *Nucl. Instrum. Methods Phys. Res. B* **175–177**, 340 (2001).
- ¹¹R. Kögler, A. Peeva, J. Kaschny, W. Skorupa, and H. Hutter, *Nucl. Instrum. Methods Phys. Res. B* **186**, 298 (2002).
- ¹²R. Krause-Rehberg, F. Börner, and F. Redman, *Appl. Phys. Lett.* **77**, 3932 (2000).
- ¹³R. Krause-Rehberg, F. Börner, F. Redman, J. Gebauer, R. Kögler, R. Kliemann, W. Skorupa, W. Egger, G. Kögel, and W. Triftshäuser, *Physica B* **308–310**, 442 (2001).
- ¹⁴R. Kögler, A. Peeva, J. Kaschny, W. Skorupa, and H. Hutter, *Solid State Phenom.* **82–84**, 399 (2002).
- ¹⁵A. Peeva, R. Kögler, and W. Skorupa, *Nucl. Instrum. Methods Phys. Res. B* (to be published).
- ¹⁶P. Leveque, H. Kortegaard Nielsen, P. Pellegrino, A. Hallen, B. G. Svesson, A. Kuznetsov, J. Wong-Leung, C. Jagadish, and V. Privitera, *J. Appl. Phys.* **93**, 871 (2003).
- ¹⁷Y. M. Gueorguiev, R. Kögler, A. Peeva, D. Panknin, A. Mücklich, R. A. Yankov, and W. Skorupa, *Appl. Phys. Lett.* **75**, 3467 (1999).
- ¹⁸Y. M. Gueorguiev, R. Kögler, A. Peeva, A. Mücklich, D. Panknin, R. A. Yankov, and W. Skorupa, *J. Appl. Phys.* **88**, 5645 (2000).
- ¹⁹M. D. Griffin, *J. Electrochem. Soc.* **138**, 1160 (1991).
- ²⁰*DIOS-ISE, ISE TCAD Release 8.0*, User's Manual, Zürich, July 2002 (<http://www.ise.ch>).
- ²¹M. Posselt, B. Schmidt, C. S. Murthy, T. Feudel, and K. Suzuki, *J. Electrochem. Soc.* **144**, 1496 (1997).
- ²²M. Posselt, L. Bischoff, and J. Teichert, *Appl. Phys. Lett.* **79**, 1444 (2001).
- ²³R. Kögler, A. Peeva, W. Anwand, P. Werner, A. B. Danilin, and W. Skorupa, *Solid State Phenom.* **69–70**, 235 (1999).
- ²⁴K. L. Beaman, J. M. Glasko, S. Koveshnikov, and G. A. Rozgonyi, *Solid State Phenom.* **69–70**, 247 (1999).
- ²⁵D. B. Lee and A. F. W. Willoughby, *J. Appl. Phys.* **43**, 245 (1972).
- ²⁶D. Lecrosnier, J. Paugam, F. Richou, G. Pelous, and F. Beniere, *J. Appl. Phys.* **51**, 1036 (1980).
- ²⁷M. Uematsu, *J. Appl. Phys.* **83**, 120 (1998).
- ²⁸S. Koveshnikov and O. Kononchuk, *Appl. Phys. Lett.* **73**, 2340 (1998).